

Crystalline electric fields and the ground state of $\text{Ce}_3\text{Rh}_4\text{Pb}_{13}$.

D. A. Sokolov¹, M. C. Aronson¹, C. Henderson², and J. W. Kampf³

¹⁾ *Department of Physics, University of Michigan,
450 Church Street, Ann Arbor, MI 48109-1040, USA*

²⁾ *Department of Geological Sciences,
University of Michigan, 1100 North University,
Ann Arbor, MI 48109-1005, USA*
and

³⁾ *Department of Chemistry,
University of Michigan, 930 North University,
Ann Arbor, MI 48109-1055, USA*

We have succeeded in synthesizing of single crystals of a new intermetallic compound, $\text{Ce}_3\text{Rh}_4\text{Pb}_{13}$. Magnetic susceptibility measurements indicate that the Ce moments are highly localized, despite the metallic character of the electrical resistivity. Heat capacity measurements reveal that the cubic crystal electric field lifts the six-fold degeneracy of the Ce^{3+} ground state, with the quartet state separated by approximately 60 K from the doublet ground state. The magnetic field dependence of the heat capacity at low temperature indicates a further splitting of the doublet, but no sign of magnetic order was found above 0.35 K.

PACS numbers: 71.20.Eh, 75.40.Cx

Rare-earth based intermetallic compounds continue to attract a great deal of interest due to the richness of the magnetic and electronic phenomena observed in these systems^{1,2}. In particular, non-Fermi liquid behavior was found in the vicinity of a zero temperature magnetic phase transitions, often manifested by power-law temperature dependences of the magnetic susceptibility and logarithmic temperature dependence of the heat capacity divided by the temperature. Synthesis of novel rare-earth intermetallics in a pure form, typically achieved by growing single crystals, is instrumental in identifying new physics associated with the magnetic ordering at zero temperature.

The compounds with a general formula $\text{R}_3\text{Rh}_4\text{Sn}_{13}$, where R is a rare-earth element, were first synthesized by Remeika *et al.*³. It was found that the materials with $\text{R}=\text{Tm}$, Lu , Y were superconductors, while compounds with $\text{R}=\text{Tb}$, Dy , Ho ordered magnetically. The $\text{R}=\text{Eu}$ member of this family demonstrated reentrant superconductivity, in turn destroyed by the onset of ferromagnetic order. Subsequently, other members of a broader family $\text{R}_3\text{T}_4\text{X}_{13}$, where $\text{T}=\text{transitional metal}$ and X is metalloid from 4th or 5th group, were studied and found to order antiferromagnetically at low temperatures^{4,5,6}. Interestingly, heavy fermion $\text{Ce}_3\text{Ir}_4\text{Sn}_{13}$ orders antiferromagnetically and demonstrates an intriguing double peak feature near ordering temperature on the temperature dependence of the heat capacity^{4,7}. In heavy fermion $\text{Ce}_3\text{Pt}_4\text{In}_{13}$, the Kondo and RKKY energy scales are nearly equivalent and their balance can be changed by the applied pressure⁸. Recently, new $\text{Ln}_3\text{Co}_4\text{Sn}_{13}$ compounds, with $\text{Ln}=\text{Ce}, \text{La}$ were reported^{9,10}. $\text{Ce}_3\text{Co}_4\text{Sn}_{13}$ is a heavy fermion, which does not order magnetically above $T \sim 0.35$ K, while its La counterpart is a conven-

tional superconductor.

Such a panorama of magnetic properties and the variety of electronic ground states in cubic $\text{R}_3\text{T}_4\text{X}_{13}$ motivated us to synthesize a new compound with $\text{T}=\text{Rh}$, and $\text{X}=\text{Pb}$. We report here a systematic study of the physical properties of a novel cubic metallic compound $\text{Ce}_3\text{Rh}_4\text{Pb}_{13}$, which we carried out in a search for new materials lying close to the quantum critical point.

Single crystals of $\text{Ce}_3\text{Rh}_4\text{Pb}_{13}$ were grown from Pb flux. Single crystal x-ray diffraction experiments were carried out at room temperature using a Bruker 1K CCD based single crystal diffractometer with $\text{Mo K}\alpha$ radiation. The structure was solved and refined using SHELXTL package¹¹. Electron microprobe measurements were performed using a Cameca SX100 microprobe spectrometer calibrated with elemental Ce, Rh, and Pb standards. The magnetic susceptibility was measured using a Quantum Design Magnetic Phenomenon Measurement System at temperatures from 1.8 K to 300 K. The electrical resistivity ρ of $\text{Ce}_3\text{Rh}_4\text{Pb}_{13}$ was measured by the conventional four-probe method between 0.35 K and 300 K in zero magnetic field. Measurements of the heat capacity were performed using a Quantum Design Physical Property Measurement System at temperatures from 0.35 K to 70 K and in magnetic fields up to 2 T.

Electron microprobe experiments found that the stoichiometry was uniform over the surface of the crystals, with the elemental ratios for $\text{Ce}:\text{Rh}:\text{Pb}$ of $3 \pm 0.02 : 4 \pm 0.04 : 13 \pm 0.02$. Single crystal X-ray diffraction experiments confirmed this stoichiometry and found a cubic structure (space group $\text{Pm}\bar{3}\text{n}$, No 223) with $a=10.0010(6)$ Å, which is shown in Fig. 1. The unit cell contains 2 formula units. Corrections were made for absorption and extinction, and the atomic positions were refined

TABLE I: Structural parameters of $\text{Ce}_3\text{Rh}_4\text{Pb}_{13}$ at 293 K. Space group $\text{Pm}\bar{3}\text{n}$; $a=10.0010(6)\text{\AA}$, $V=1000.30(10)\text{\AA}^3$, calculated density 11.705 g/cm^3 . Agreement indices: $R_1=0.0398$, $wR_2=0.1158$, goodness of fit 1.256.

Atom	Site	x	y	z	$U_{eq}^a (\text{\AA}^2)$
Pb(1)	2a	0	0	0	0.027(1)
Pb(2)	24k	0.1557(1)	0.3070(1)	0	0.024(1)
Ce	6d	0	0.5	0.25	0.023(1)
Rh	8e	0.25	0.25	0.25	0.020(1)

^a U_{eq} is defined as one-third of the trace of the orthogonalized U_{ij} tensor.

TABLE II: Selected bond lengths (\AA) in $\text{Ce}_3\text{Rh}_4\text{Pb}_{13}$ at 293 K.

Ce-Pb(1)	5.591(1)	Ce-Pb(2)($\times 8$)	3.5220(7)
Ce-Pb(2)($\times 4$)	3.4897(9)	Ce-Rh	3.5359(2)
Rh-Pb(2)	2.7321(4)	Rh-Pb(1)	4.331(1)
Pb(1)-Pb(2)	3.4423(10)	Pb(2)-Pb(2)	3.3182(15)
Pb(1)-Pb(1)	8.661(1)		

with anisotropic displacement parameters. The results of the X-ray diffraction experiments are summarized in Tables I,II.

The temperature dependence of the electrical resistivity ρ is that of a good metal, Fig. 2. ρ decreases from the value of $100\text{ }\mu\Omega\cdot\text{cm}$ at 300 K to $\sim 30\text{ }\mu\Omega\cdot\text{cm}$ at 2 K. The inset to Fig. 2 shows a partial superconducting transition at $T_c=2\text{ K}$, which we believe is due to trace amounts of superconducting RhPb_2 ¹². Measurements of the Meissner effect confirmed these conclusions, finding a

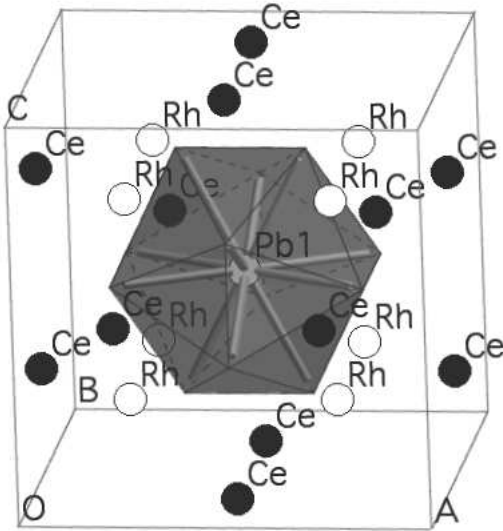


FIG. 1: Crystal structure of $\text{Ce}_3\text{Rh}_4\text{Pb}_{13}$. Single unit cell is shown highlighting the Pb1(Pb2)_{12} icosahedron (light grey).

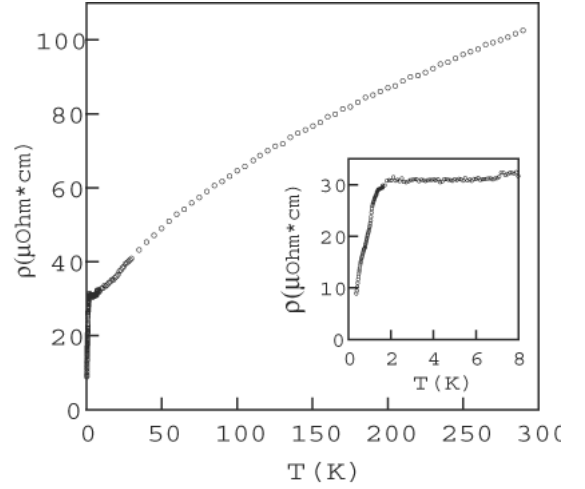


FIG. 2: Temperature dependence of the electrical resistivity of $\text{Ce}_3\text{Rh}_4\text{Pb}_{13}$.

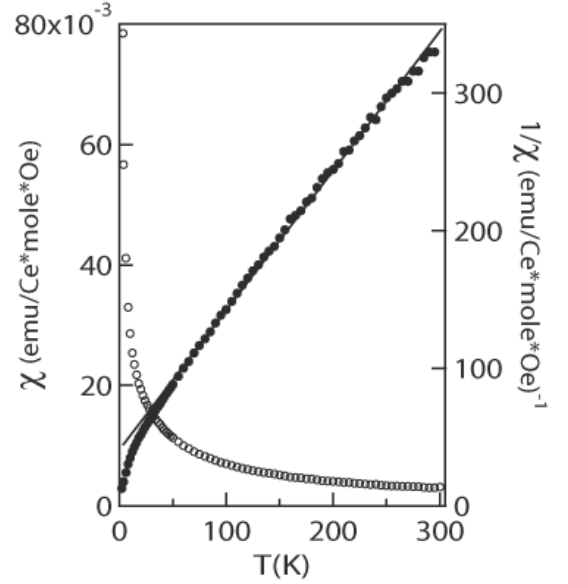


FIG. 3: Temperature dependence of the magnetic susceptibility (\circ) and its inverse (\bullet) of $\text{Ce}_3\text{Rh}_4\text{Pb}_{13}$ measured in 1000 Oe.

volume fraction of less than 1% for the proposed RhPb_2 inclusions.

Measurements of the magnetic susceptibility found that the Ce ions in $\text{Ce}_3\text{Rh}_4\text{Pb}_{13}$ are well localized. The temperature dependence of the dc magnetic susceptibility χ and its inverse are shown in Fig. 3. χ decreases monotonically with decreasing temperature, and the inverse of χ was fitted to a straight line between 34 K and 300 K, Fig. 3. The fit yielded a Weiss temperature $\Theta=-39\text{ K}\pm 0.7\text{ K}$, suggesting that the magnetic correlations in $\text{Ce}_3\text{Rh}_4\text{Pb}_{13}$ are antiferromagnetic, and an effective magnetic moment $\mu_{eff}=2.6\pm 0.1\text{ }\mu_B$ per Ce ion, close to the $2.54\text{ }\mu_B$ expected for a free Ce^{3+} ion. Below $\sim 30\text{ K}$ $1/\chi$ demonstrates a pronounced downward curvature, as

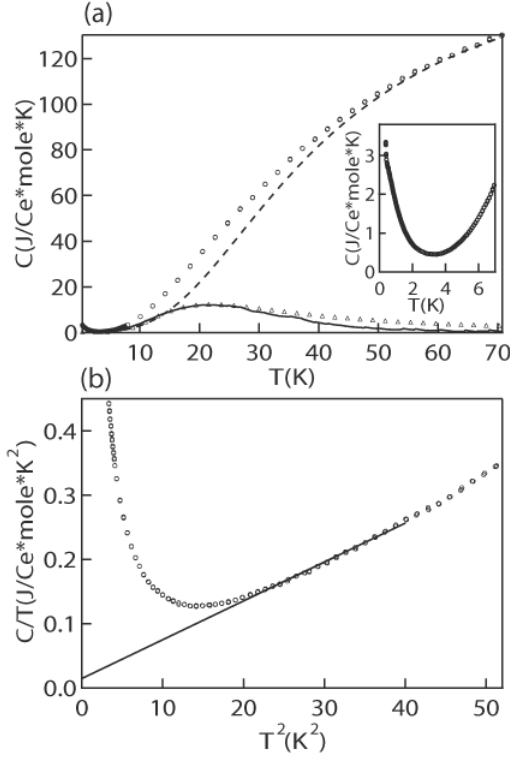


FIG. 4: (a) Temperature dependence of the heat capacity C (\circ) of $\text{Ce}_3\text{Rh}_4\text{Pb}_{13}$ measured in zero field. The dashed line is the estimated lattice heat capacity. Δ mark the electronic and magnetic parts of the total heat capacity. The solid line is the Schottky fit. (b) The electronic part of the heat capacity $C_{el} = \gamma T$ is determined from this plot of $C/T = \gamma + \beta T^2$.

is characteristic of systems with a substantial crystalline electric field (CEF) splitting of the ground state of Ce^{3+} . χ is found to be completely isotropic in the measured temperature range, which is expected for a cubic system such as $\text{Ce}_3\text{Rh}_4\text{Pb}_{13}$ where Ce ions occupy only equivalent sites in the unit cell.

Heat capacity measurements confirm that the Ce moments are only weakly coupled to the conduction electrons. The temperature dependence of the heat capacity $C(T)$ was measured in zero field and at temperatures as large as 70 K (Fig. 4a). We have estimated the phonon contribution to the heat capacity C_{ph} using the Debye expression and a Debye temperature $\theta_D = 163 \pm 10$ K. C_{ph} is subtracted from $C(T)$ in Fig. 4a to isolate the remaining magnetic and electronic contributions to the heat capacity. The latter is expected to result in a component of the heat capacity which is linear in temperature, $C_{el} = \gamma T$.

C/T is plotted as a function of T^2 in Fig. 4b, demonstrating that the electronic contribution is found only over a narrow range of temperatures, yielding $\gamma = 15 \pm 2$ mJ/moleK². We conclude that the purely electronic contribution to the heat capacity is very small, as would be expected for weakly correlated conduction electrons or alternatively for a low density of conduction electrons for $\text{Ce}_3\text{Rh}_4\text{Pb}_{13}$. In either case, we conclude that the Kondo

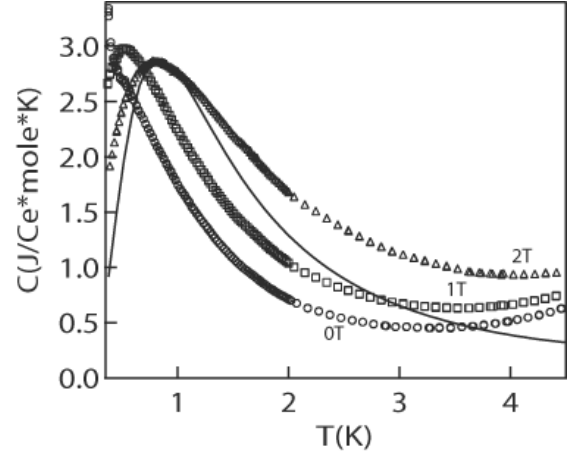


FIG. 5: Temperature dependence of the heat capacity of $\text{Ce}_3\text{Rh}_4\text{Pb}_{13}$ measured in 0 T (\circ), 1 T (\square) and 2 T (Δ). Solid line is the Schottky fit.

temperature for this system is very small.

The crystal electric field scheme for these localized Ce moments was established from heat capacity measurements. The CEF of a cubic symmetry splits the ground state manifold of Ce^{3+} ions with a total angular momentum $J = 5/2$, into a doublet and a quartet¹³. We suggest that the broad maximum found in $C - C_{ph} = C_{mag}$ near 23 K in Fig. 4a is a Schottky anomaly, which corresponds to a thermally activated transition from a Γ_7 doublet ground state to the higher lying Γ_8 quartet, separated by an energy gap of 60 K. Therefore, the full Ce^{3+} moment can only be found above 60 K. Below ~ 60 K we expect to find a reduced and temperature dependent effective magnetic moment.

Given the high crystal symmetry, the relatively close Ce-Ce spacing and the absence of a measurable Kondo effect, we searched for evidence that magnetic order occurs in this system. At temperatures below 3 K the heat capacity demonstrates a monotonic increase, perhaps indicative of incipient order, shown in the inset of the Fig. 4a. However, the application of a magnetic field shows that this is the high temperature side of another broad Schottky peak. When magnetic field is applied to $\text{Ce}_3\text{Rh}_4\text{Pb}_{13}$, the upturn develops into a broad maximum, which shifts to higher temperatures with increasing field, Fig. 5. The best fit to the pronounced maximum found in the 2 T data was obtained assuming the Schottky-type transition between the levels with the same degeneracies. A magnetic field of 2 T splits the ground state doublet into two singlets separated by an energy gap of 2 K, indicating that the low-lying doublet ground state is itself split, with an extrapolated energy gap of ~ 1 K in zero field.

The temperature dependence of the entropy calculated from the heat capacity data of Fig. 4a is shown in Fig. 6. The entropy increases sharply up to $T = 2$ K and almost saturates at the value of $\sim 0.62 \ln 2$ and increases as the temperature is further increased. The slow approach of

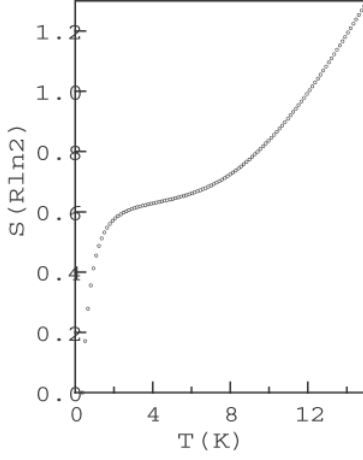


FIG. 6: Temperature dependence of the zero field entropy of $\text{Ce}_3\text{Rh}_4\text{Pb}_{13}$.

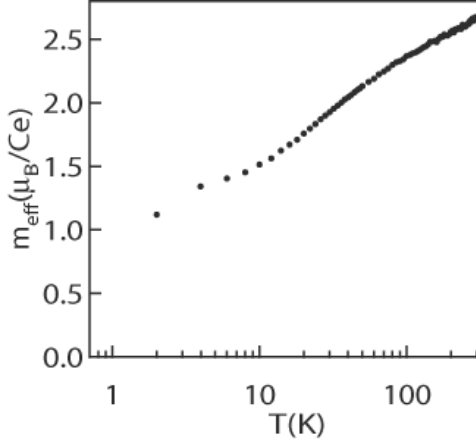


FIG. 7: Temperature dependence of the effective magnetic moment $\mu_{eff}(T) = \sqrt{\frac{3k_B T \chi}{N}}$ of $\text{Ce}_3\text{Rh}_4\text{Pb}_{13}$.

the entropy to the expected value of $R \ln 2$ is likely due in part to the further splitting of the ground doublet, but may also reveal the onset of a weak Kondo effect, with a Kondo temperature of no more than 1-2 K.

The temperature dependence of the magnetic susceptibility χ is in good agreement with the crystal field scheme deduced from the heat capacity measurements in $\text{Ce}_3\text{Rh}_4\text{Pb}_{13}$. Fig. 7 shows the temperature dependence of the effective magnetic moment defined as $\mu_{eff}(T) = \sqrt{\frac{3k_B T \chi}{N}}$. Well above $T=60$ K, which is the energy splitting between the ground state doublet and the excited quartet split by the CEF, μ_{eff} is close to the value of $2.54 \mu_B$ expected for a free Ce^{3+} ion. At lower temperatures CEF partially lifts the degeneracy of the ground state and reduces the total angular momentum J . This, in turn, lowers the μ_{eff} as $\mu_{eff} \propto \sqrt{J(J+1)}$.

The derived CEF allows us to calculate the CEF magnetic susceptibility χ_{CEF} considering both the Curie and Van-Vleck terms. We have used the eigenfunctions re-

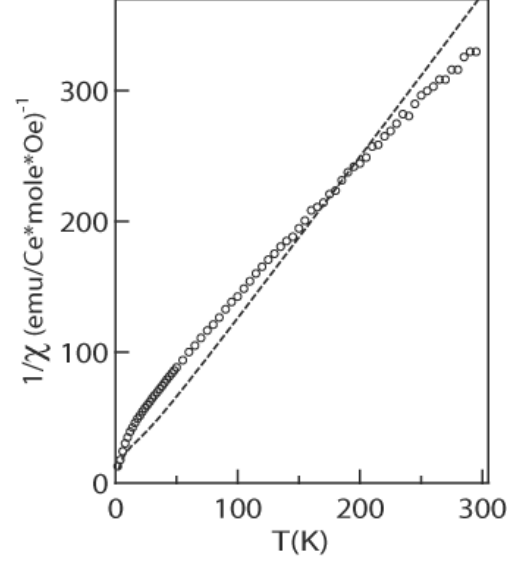


FIG. 8: Temperature dependence of the inverse of the magnetic susceptibility (\circ) of $\text{Ce}_3\text{Rh}_4\text{Pb}_{13}$ and the inverse of the calculated χ_{CEF} .

ported in Ref.¹³:

$$\begin{aligned} \text{for } \Gamma_7: & \frac{1}{\sqrt{6}}|\pm 5/2\rangle - \sqrt{5/6}|\mp 3/2\rangle \\ \text{for } \Gamma_8: & \sqrt{5/6}|\pm 5/2\rangle + \frac{1}{\sqrt{6}}|\mp 3/2\rangle \text{ and } |\pm 1/2\rangle. \end{aligned}$$

$$\chi_{CEF} = \frac{(g_J \mu_B)^2}{1+2e^{-\Delta/k_B T}} \left(\frac{\frac{25}{36} + \frac{65}{18}e^{-\Delta/k_B T}}{k_B T} + \frac{40(1-e^{-\Delta/k_B T})}{9\Delta} \right), \quad (1)$$

Fig. 8 shows the inverse of χ and χ_{CEF} . We note that the agreement between χ_{CEF} and χ is reasonable.

Taken together, our data reveal $\text{Ce}_3\text{Rh}_4\text{Pb}_{13}$ to be an almost completely localized moment system, with no indication of magnetic order above 0.35 K, and a similarly small Kondo temperature. We infer that $\text{Ce}_3\text{Rh}_4\text{Pb}_{13}$ most likely lies at the weakly coupled extreme of the Doniach phase diagram¹⁴, although we cannot entirely rule out the possibility that it is very close to the quantum critical point, where both the magnetic ordering and Kondo temperatures can vanish simultaneously. Our data suggest that despite high crystal symmetry and closely spaced Ce moments, $\text{Ce}_3\text{Rh}_4\text{Pb}_{13}$ apparently avoids magnetic order through the successive lifting of the Ce degeneracy, and the consequent suppression of the Ce moment. It will be very interesting to extend our measurements to temperatures below 0.4 K to ascertain the ultimate fate of $\text{Ce}_3\text{Rh}_4\text{Pb}_{13}$: magnetic order, Kondo lattice formation, or even superconductivity.

Work at the University of Michigan was performed under grant NSF-DMR-0405961.

-
- ¹ G. R. Stewart, *Rev. Mod. Phys.* **73**, 797 (2001).
- ² Y. Ōnuki, R. Settai, K. Sugiyama, T. Takeuchi, T. C. Kobayashi, Y. Haga, E. Yamamoto, *J. Phys. Soc. Jpn* **73**, 769 (2004).
- ³ J. P. Remeika, G. P. Espinosa, A. S. Cooper, H. Barz, J. M. Rowell, D. B. McWhan, J. M. Vandenberg, D. E. Moncton, Z. Fisk, L. D. Woolf, H. C. Hamaker, M. B. Maple, G. Shirane and W. Thomlinson, *Solid State Commun.* **34**, 923 (1980).
- ⁴ S. Takayanagi, H. Sato, T. Fukuhara, N. Wada, *Physica B* **199 + 200**, 49 (1994).
- ⁵ Yuji Aoki, Tadashi Fukuhara, Hitoshi Sugawara and Hideyuki Sato, *J. Phys. Soc. Jpn* **65**, 1005 (1996).
- ⁶ Chiyoko Nagoshi, Ryunosuke Yamamoto, Keitaro Kuwahara, Hajime Sagayama, Daich Kawana, Masahumi Kongi, Hitoshi Sugawara, Yuji Aoki, Hideyuki Sato, Tetsuya Yokoo and Masatoshi Arai, *J. Phys. Soc. Jpn* **75**, 044710 (2006).
- ⁷ C. Nagoshi, H. Sugawara, Y. Aoki, S. Sakai, M. Kohgi, H. Sato, T. Onimaru, T. Sakakibara, *Physica B* **359 – 361**, 248 (2005).
- ⁸ M. F. Hundley, J. L. Sarrao, J. D. Thompson, R. Movshovich, and M. Jaime, C. Petrovic and Z. Fisk, *Phys. Rev. B*, **65**, 024401 (2001).
- ⁹ Evan Lyle Thomas, Han-Oh Lee, Andrew N. Bankston, Samuel MaQuilon, Peter Klavins, Monica Moldovan, David P. Young, Zachary Fisk, Julia Chan, *J. Solid State Chem.* **179**, 1642 (2006).
- ¹⁰ A. L. Cornelius, A. D. Christianson, J. L. Lawrence, V. Fritsch, E. D. Bauer, J. L. Sarrao, J. D. Thompson, P. G. Pagliuso, *Physica B* **378 – 380**, 113 (2006).
- ¹¹ G. M. Sheldrick, SHELXTL v. 6.12 Bruker Analytical X-ray (Madison, WI, 2001).
- ¹² M. F. Gendron and R. E. Jones, *J. Phys. Chem. Solids.* **23**, 405 (1962).
- ¹³ K. R. Lea, M. J. Leask, and W. P. Wolf, *J. Phys. Chem. Solids* **23**, 1381 (1962).
- ¹⁴ S. Doniach, *Physica (Amsterdam)* **91B + C**, 231 (1977).